Available online at www.sciencedirect.com
ScienceDirect
Polymer 48 (2007) 264–269
polymer
www.elsevier.com/locate/polymer

Aliphatic acid esters of (2-hydroxypropyl) cellulose—Effect of side chain length on properties of cholesteric liquid crystals

Bin Huang [a], Jason J. Ge [b,1], Yonghong Li [a], Haoqing Hou [a,*]

[a] College of Chemistry and Chemical Engineering, Jiangxi Normal University, 99 Ziyang Street, Nanchang, Jiangxi 330022, China
[b] Maurice Morton Institute and Department of Polymer Science, University of Akron, Akron, OH 44325-3909, USA

Received 13 August 2006; received in revised form 12 November 2006; accepted 15 November 2006
Available online 4 December 2006

Abstract

A series of aliphatic acid esters of (2-hydroxypropyl) cellulose (C_nPC) were synthesized via the esterification of aliphatic acid chloride and (2-hydroxypropyl) cellulose (HPC). The liquid crystalline (LC) phases and transitions were investigated using differential scanning calorimetry, wide-angle X-ray diffraction (WAXD), and polarized light microscope (PLM) techniques. This series of C_nPC polymers exhibited characteristic features of cholesteric LC phases between their glass transition and isotropization temperatures. The cholesteric LC characteristics were studied utilizing an ultraviolet/visible/near infrared spectrometer in a reflection mode. It was confirmed that, with an increase in the number of methylene units in the side chains of this series of C_nPC polymers, there was an increase, on the scale of nanometers, in the layer spacing values for the cholesteric LC phases measured by WAXD. This periodic layer spacing represents the thickness of the neighboring twisted layers in a helical structure. Based on a unique significant red shift of the maximum reflection peak for the LC phases in this series of C_nPCs, it is evident that the pitch distance in the helical structure also increases with an increase in the length of methylene units in the side chains.

Keywords: Cholesteric liquid crystal; Cellulose derivative; Side chain

1. Introduction

Cholesteric liquid crystals (ChLCs) are of great scientific and technological interest due to their unique selective reflection of light at characteristic wavelengths with a specific pitch distance. Important applications of ChLCs have been identified, including rigid or flexible reflective liquid crystal displays and reflective polarization films for use in flat panel displays to improve brightness [1–4]. The selective reflection ($\lambda = nP_o\cos\theta$) is caused by the molecular helical structure with a pitch distance (P_o) in cholesteric liquid crystalline (ChLC) phases where the average refractive index (n) is equal to $[(n_{\parallel}^2 + 2n_{\perp}^2)/3]^{0.5}$ and the incident angle is θ [1]. Interestingly, most of the cellulose derivatives form cholesteric LC phases in solutions within certain concentration regions (lyotropic) or in the bulk within certain temperature regions (thermotropic) [5–18]. Generally speaking, it is understood that physical packing (chiral arrangement) schemes of stiff cellulose chains could be considered playing important roles in inducing the formation of cholesteric LC phases. In particular, when the flexible side chains are connected onto the cellulose backbones, the resulting hairy-rod cellulose polymers start forming these cholesteric LC phases. It is believed that the attachment of flexible side chains onto the rigid cellulose molecules can facilitate the orientational order of the semi-rigid hairy-rod backbones with side chains with increasing the chain mobility and enhancing the solubility. Among the cellulose derivatives, (2-hydroxypropyl) cellulose (HPC) derivatives are of specific interest because they can form either cholesteric lyotropic or thermotropic LC phases [18–24]. A particularly interesting property of the cellulose derivatives is that, based on different chemical structures, the materials can reflect light at a specific light wavelength and in a specific temperature region. For

* Corresponding author. Tel.: +86 791 8120389; fax: +86 791 8120536.
E-mail address: haoqing@jxnu.edu.cn (H. Hou).
[1] Present address: Altuglas International, Arkema, 900 1st Avenue, King of Prussia, PA 19403, USA.

0032-3861/$ - see front matter © 2006 Elsevier Ltd. All rights reserved.
doi:10.1016/j.polymer.2006.11.033

example, (2-ethoxypropyl) cellulose (EPC) [15] reflects visible light at 130–160 °C, while (2-acetoxy-propyl) cellulose (C_2PC) [18], [(2-propionyloxy)-propyl] cellulose (C_3PC) [19] and [(2-butyrionyloxy)propyl] cellulose (C_4PC) [24] display iridescent color at ambient temperature due to the selective reflections of light from the cholesteric LC phases.

One of the most important approaches towards obtaining cellulose derivatives exhibiting cholesteric LC phase transitions is via the esterification of HPC [19,24]. These cellulose derivatives can possess different side chain lengths based on different numbers of methylene units. The motivation of this work is to design a series of HPC derivatives (C_nPC, $n = 5$, 6, 7 and 10) to further improve the systematic understanding of the side chain effect on the formation of thermotropic cholesteric LC phases and phase transitions as well as their unique selectivity for color reflections and the pitch distance in the cholesteric LC phases.

2. Experimental part

2.1. Materials

2-Hydroxylpropyl cellulose (HPC) (Aldrich, weight average molecular weight, $M_w = 100{,}000$ g/mol) was dried at 50 °C (30 mbar) prior to use. Aliphatic acid chloride ($CH_3(CH_2)_{n-2}COCl$, $n = 2$, 3, 4, 5, 6, 7, 10, purchased from Aldrich) was used as received. Acetone (Aldrich) was dried over $CaCl_2$ for 2 days and was distilled in an N_2 atmosphere before use.

The synthetic procedure of C_nPC is described here using C_5PC as an example. HPC of 5.0 g (corresponding to 41.71 mmol of hydroxyl groups) was added to 30 mL acetone under a dry nitrogen atmosphere and was dissolved by heating the solution. Then 15.1 mL (125.13 mmol) valeric acid chloride was swiftly added to the solution of HPC by using a syringe. After 2 h of reflux, the reaction mixture was poured into 200 mL distilled water. After removing the liquid phase, a cream-colored, sticky material was obtained and then dissolved in 80 mL acetone and precipitated by adding 5 mL of water to the solution. The pasty product was liberated from the acetone/water by decantation. The second solution precipitation was repeated for 5 times. Finally, the product was dried at 60 °C (30 mbar, 48 h). The amount of 6.57 g of the final polymer material was obtained with a yield of 76.8%.

Gel permeation chromatographic (GPC) results showed that $M_w = 6.83 \times 10^4$. The degree of substitution (DS) [23] was determined as 2.67 by ^{1}H nuclear magnetic resonance (NMR) and as 2.79 by saponification. Infrared (IR) spectroscopic results showed absorption at 3300–3600 cm^{-1} for –OH stretching, 2850–3000 cm^{-1} for the C–H stretching, and 1731.2 cm^{-1} for the C=O stretching. The results obtained in ^{1}H NMR (in $CDCl_3$) analysis are 2.8–4.5 ppm for the protons of the anhydroglucose ring; 4.95 ppm for @-$OCH_2CH(CH_3)[OCH_2CH(CH_3)$-$(OOC(CH_2)_3CH_3)]$; 3.48 ppm for @-$OCH_2CH(CH_3)[OCH_2CH$-$(CH_3)(OOC(CH_2)_3CH_3)]$; 1.08 ppm for @-$OCH_2CH(CH_3)$-$[OCH_2CH(CH_3)(OOC(CH_2)_3CH_3)]$; 2.23 ppm for @-$OCH_2CH$-$(CH_3)[OCH_2CH(CH_3)(OOCCH_2CH_2CH_2CH_3)]$; 1.63 ppm for @-$OCH_2CH(CH_3)[OCH_2CH(CH_3)(OOCCH_2CH_2CH_2CH_3)]$; 1.29 ppm for @-$OCH_2CH(CH_3)[OCH_2CH(CH_3)(OOCCH_2CH_2$-$CH_2CH_3)]$; 0.92 ppm for @-$OCH_2CH(CH_3)[OCH_2CH(CH_3)$-$(OOCCH_2CH_2CH_2CH_3)]$; 1.17 ppm for @-$OCH_2CH(CH_3)$-$[OCH_2CH(CH_3)(OOCCH_2CH_2CH_2CH_3)]$ (@ stands for the structure of cellulosic chain).

The rest of the C_nPC polymers with different lengths in the side chains were synthesized using the same procedure as described for C_5PC, similar to Refs. [18,24]. Molecular weight values and yields are given in Table 1.

2.2. Equipments and experiments

Infrared (IR) spectroscopy was performed using a Perkin Elmer FT-IR 1600 in a transmission mode. The samples were dissolved in $CHCl_3$ at the concentration of 5% and then solution cast onto KBr plates. The IR spectra were recorded after the solvent was evaporated completely. Solution ^{1}H NMR spectra (400 MHz) were recorded on a Bruker AC 400 while the samples were dissolved in $CDCl_3$ at room temperature. Differential scanning calorimetric (DSC) measurements were conducted on pasty samples using A Mettler-30 DSC in standard aluminum pans with a cooling rate of 15 °C/min from the isotropic melt. Polarizing light microscopy (PLM) was performed using a Leitz Orthoplan microscope equipped with a Mettler FP hot stage. The PLM samples were prepared in the form of film with about 1 mm thickness by, respectively, putting 0.5 g of each C_nPC pasty product on a clean glass slide and keeping the slides with C_nPC samples in a baking oven at 60 °C overnight for making the sample thickness more uniform and for developing LC phases. Gel permeation chromatography (GPC) was carried out using a Viscotek detector and a set of 5 mm mixed bead columns. The calibration was done with a series of standard polystyrenes with known molecular weight. The samples were dissolved in tetrahydrofuran (THF) at ambient temperature and filtrated with a 0.4 μm PTFE membrane filter. Wide-angle X-ray diffraction (WAXD) experiments were conducted using a Siemens D5000 (Cu Kα). The pasty samples were used in WAXD experiments in a reflection mode. The samples were prepared in the way of preparing PLM samples. The UV/vis/

Table 1
Reaction conditions, yield, degree of substitution, and molecular weight for C_nPCs

	Time (h)	$C_{n-1}COCl$ (mL)	Yield[a] (%)	DS[b]	DS[c]	M_w ($\times 10^4$)	M_w/M_n
C_2PC	2	9.1	70.7	2.70	2.82	9.62	2.63
C_3PC	2	11.5	72.0	2.69	2.83	7.80	1.27
C_4PC	2	13.3	77.5	2.67	2.80	8.65	1.43
C_5PC	2	15.2	76.8	2.64	2.79	6.83	1.24
C_6PC	2	17.7	79.0	2.59	2.78	6.38	1.47
C_7PC	2	19.6	78.5	2.64	2.76	6.38	1.37
C_{10}PC	2	26.5	80.6	2.65	2.81	7.06	1.56

[a] Yield was calculated on the basis of 100% esterification of HPC with DE of 3.4.
[b] Degree of substitution (DS) was determined by NMR [23].
[c] Determined by saponification [23].

NIR optical spectra were recorded on a Perkin Elmer Lambda 19 UV/vis/NIR photospectrometer with an integrating sphere detector in a reflection mode where the film samples were prepared like the PLM samples by using about 0.1 g C_nPC product for each sample but for C_6PC using 0.5 g. The refractive index of the polymer films was measured with a Metricon 2010 optical prism coupler at a wavelength of 632.8 nm. The polymer films (at the thickness of 2–5 μm) were formed by a squeeze of quartz prism on the C_nPC pasty mass on clean Si wafer substrates while the measurement was being conducted.

3. Results and discussion

3.1. Molecular structure and chain packing

Theoretically, the esterification of HPC is of molecular weight accretion. However, the data of molecular weights shown in Table 1 indicate that the M_w values of C_nPC measured in THF using GPC are lower than that of HPC (100,000 g/mol) before the esterification reactions. This deviation could come from the difference in solubility and hydrodynamic volumes of more rigid HPC and less rigid C_nPC molecules. This could also imply that the backbones of the cellulose derivatives may suffer from chain scissions during the esterification in acetone. For a C_nPC molecular structure, the −OH groups of HPC have been substituted by the aliphatyloxy groups (RCOO−) after the esterification reaction. The molecular structure of HPC has been described in previous publications [18,19,24]. Gray et al. [18] illustrated the molecular structure of C_nPC on the basis of the idealized molecular structure, as shown in Fig. 1. In this idealized structure, every anhydroglucose unit contains three flexible aliphatic ester side chains. The long backbone consists of cyclic rings with three flexible, pendent side chains. The overall chain structure becomes semi-rigid; therefore, thermotropic or lyotropic cholesteric LC phases may be developed in bulk or in high C_nPC concentration solutions.

The chain packing scheme of the thermotropic LC phase in C_nPCs can be deduced based on structural characterization methods such as the WAXD technique. Fig. 2 shows a set of one-dimensional WAXD patterns detected at room temperature for this series of C_nPCs with different numbers of methylene units in the side chains. An intense diffraction

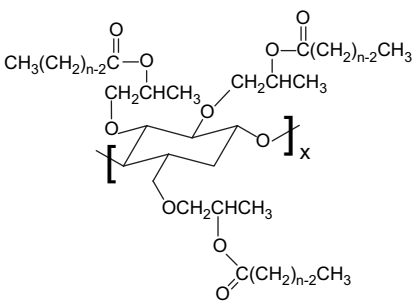

Fig. 1. An idealized chemical structure of C_nPC with three substituents [18].

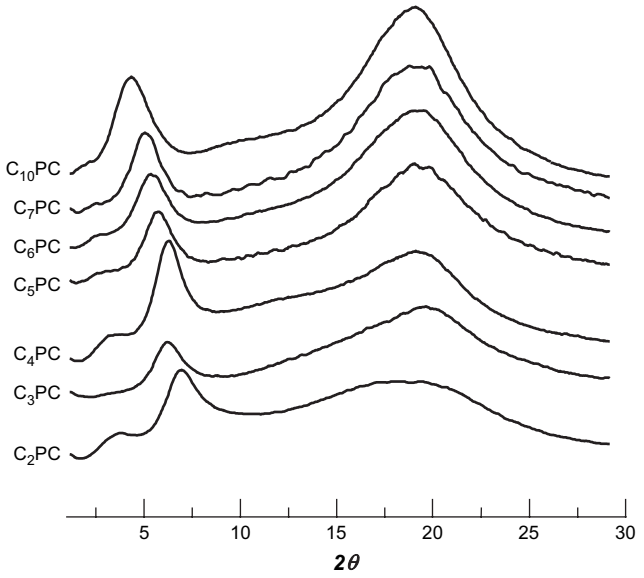

Fig. 2. 1D WAXD powder diagram: C_nPC bulk at room temperature on a glass slide in a reflection mode.

peak was observed in the low 2θ angle region between 3° and 8° in each WAXD sample. Furthermore, with increasing the number of methylene units, the d-spacing of the diffraction peak increases from 1.20 nm in C_2PC to 1.37 nm in C_5PC to 1.86 nm in C_{10}PC, as listed in Table 2. These diffraction peaks represent the existence of short range or quasi-long-range positional order. The physical origin of these diffraction peaks is associated with the smectic layered structure in LC phases although we do not know whether it belongs to smectic A (a layer normal along the fiber direction in the oriented fiber pattern) or smectic C (a layer normal tilt to the fiber direction). It is very interesting to determine the packing structure in the real space in three dimensions in our future work. Besides, the scattering halos at around $2\theta = 20°$ (d-spacing of 0.444 nm) are related to the average lateral distance between the neighboring chains. With increasing the length of methylene units, the birefringence (Δn) of C_nPC starts to decrease gradually, in which the birefringence ($\Delta n = n_{(TM)} - n_{(TE)}$) is measured at 633 nm from the difference between the TM (out-of-plane) and TE (in-plane) modes. The average refractive index of C_2PC is 1.4682 slightly higher than the others while the rest

Table 2
Physical properties of C_nPCs

C_nPC	n	Birefringence $\Delta n \times 10^3$	λ_{max} (nm)	P_o (nm)	d-Spacing (nm)
C_2PC	1.4682	4.5			1.197
C_3PC	1.4647	4.2	284	193.9	1.281
C_4PC	1.4639	3.3	405	276.7	1.323
C_5PC	1.4653	3.1	673	459.3	1.374
C_6PC	1.4647	2.2	1440	983.1	1.480
C_7PC	1.4637	2.0	1861	1271.4	1.550
			1827	1248[a]	
C_{10}PC	1.4643	1.0	2574	1758[a]	1.860

[a] Calculated on the basis of the layer line interval distance of fingerprint texture and magnification.

of them are more or less constant. Both of the reflection peak wavelengths (λ_{max}) at the maximum height and the pitch distance ($P_o = \lambda/n$) increase with the increase in the length of methylene units, which will be further discussed later.

3.2. Thermal transition properties

Fig. 3 shows a set of DSC cooling diagrams for this series of C_nPCs. It is evident that by increasing the length of the side chains, both the ΔH_i and T_i decrease. The transition enthalpy changes (LC phase to the isotropic melt, ΔH_i) and the LC phase to the isotropic melt transition temperatures (T_i) of this series of C_nPC are listed in Table 3. These important experimental results indicate that not only the backbones but also the side chains are involved in these transitions; the transitions are dependent on the length of the side chains significantly. Further cooling leads to a vitrification of the materials (as shown in Fig. 3). The glass transition temperature (T_g) of C_nPC also decreases as the number of methylene units in the side chains increases. All these observations of the thermal properties in this series of C_nPCs indicate that the methylene units in the side chains not only serve as "diluents" but also involve in these phase transitions by providing contributions to the enthalpy of the isotropic melt to LC phase transitions. Besides, these methylene units of C_nPC affect the T_g while the T_g drops with the increase in the length of the methylene units. Furthermore, the temperature range between the T_i and the T_g of the LC phase becomes narrower with an increase in the side chain length. Based on all of the side-chain dependent thermal behaviors (T_g, T_i, and $T_i - T_g$), it is clearly predicted that not only the backbones but also the side chains are involved in the formation of the LC phases and phase transitions. It is important to know from ^{13}C solid-state NMR experiments whether the molecular motion of the side chain involvement is cooperative with the backbone in the future work.

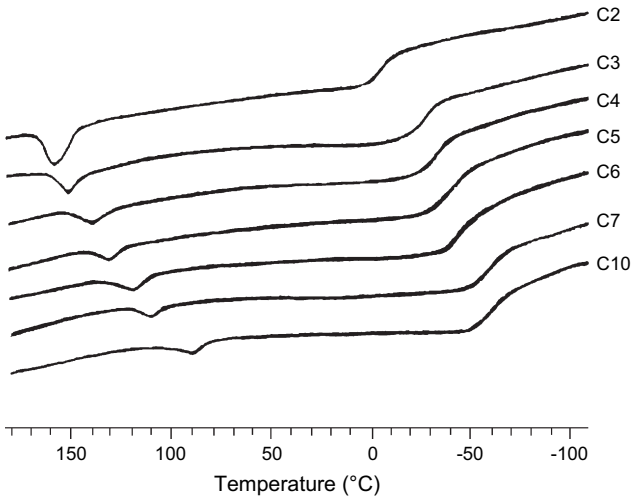

Fig. 3. DSC cooling curves of C_nPC recorded at 15 K/min and normalized per gram of material.

Table 3
Thermal properties of C_nPCs

C_nPC	T_g[a] (°C)	ΔH_i[a] (J/g)	T_i[a] (°C)	T_i[b] (°C)
C_2PC	−10.2	3.5	162.0	158–165
C_3PC	−25.8	2.8	153.5	150–158
C_4PC	−34.0	2.3	143.0	139–147
C_5PC	−44.7	1.9	130.0	126–134
C_6PC	−48.7	1.8	124.0	119–128
C_7PC	−59.3	1.7	115.0	111–120
C_{10}PC	−63.3	1.4	89.0	86–95

[a] Determined by DSC.
[b] Determined by polarized microscope with a Mettler FP hot stage.

3.3. Cholesteric LC characteristics

In order to determine the phase structures of the LC phase in this series of C_nPCs, combined characterization methods will be utilized. In addition to WAXD experiments, we choose the optical PLM methods to characterize the related phase morphology. By outward appearance, C_2PC [18] and C_3PC [19] are colorless; while C_4PC [24] and C_5PC present bright blue-purple and red prevailing color, respectively. The rest of C_nPCs (with $n = 6$, 7, and 10) are colorless sticky fluids with high viscosities at room temperature. Under PLM, all these C_nPC samples displayed the birefringence and typical LC textures from anisotropic LC materials when the samples were assembled between two glass slides. The data in Table 3 show that the birefringence in the cholesteric LC phases measured at the wavelength of 632.8 nm decreases with increasing the number of methylene unit in the side chains.

The polymers C_3PC, C_4PC, C_5PC, and C_6PC show typical 4-brush and/or 2-brush Schlieren textures at room temperature, as shown in Fig. 4a and 4b, representing the formation of the low-ordered liquid crystal phases. The C_7PC exhibits fine fingerprint textures superimposed with a Schlieren texture with 2-brush defects (Fig. 4c); while C_{10}PC shows a fingerprint textures superimposed with a Schlieren texture with 4-brush and 2-brush defects as shown in Fig. 4d. Under a mechanical shear force at elevated temperature, all of the C_nPCs present typical banded textures in which the alternating bands at scale of about 5–10 μm are perpendicular to the shear direction. This is a typical feature of the low-ordered LC phases (Fig. 4e for C_6PC). At 150 °C, a Schlieren texture of C_2PC retains before the isotropic melt (shown in Fig. 4f).

We previously reported on the formation of the cholesteric LC phase in C_4PC with a maximum reflection peak wavelength [24]. Here, we find that C_3PC, C_4PC, and C_5PC (with approximately equal DS) also displayed cholesteric selective reflections from the UV region to the visible region at room temperature. The maximum reflection peak wavelength increases when the number of methylene units in the side chains increases (Fig. 5). The C_2PC shows a cholesteric reflection at higher temperature as described previously [18]. Cholesteric reflection peaks for C_3PC, C_4PC, C_5PC and C_6PC film samples were measured using UV/vis/NIR photospectrometer in a reflection mode at room temperature with 0.2-mm thick (C_3PC, C_4PC, C_5PC) and 1-mm thick (C_6PC) samples on glass substrates.

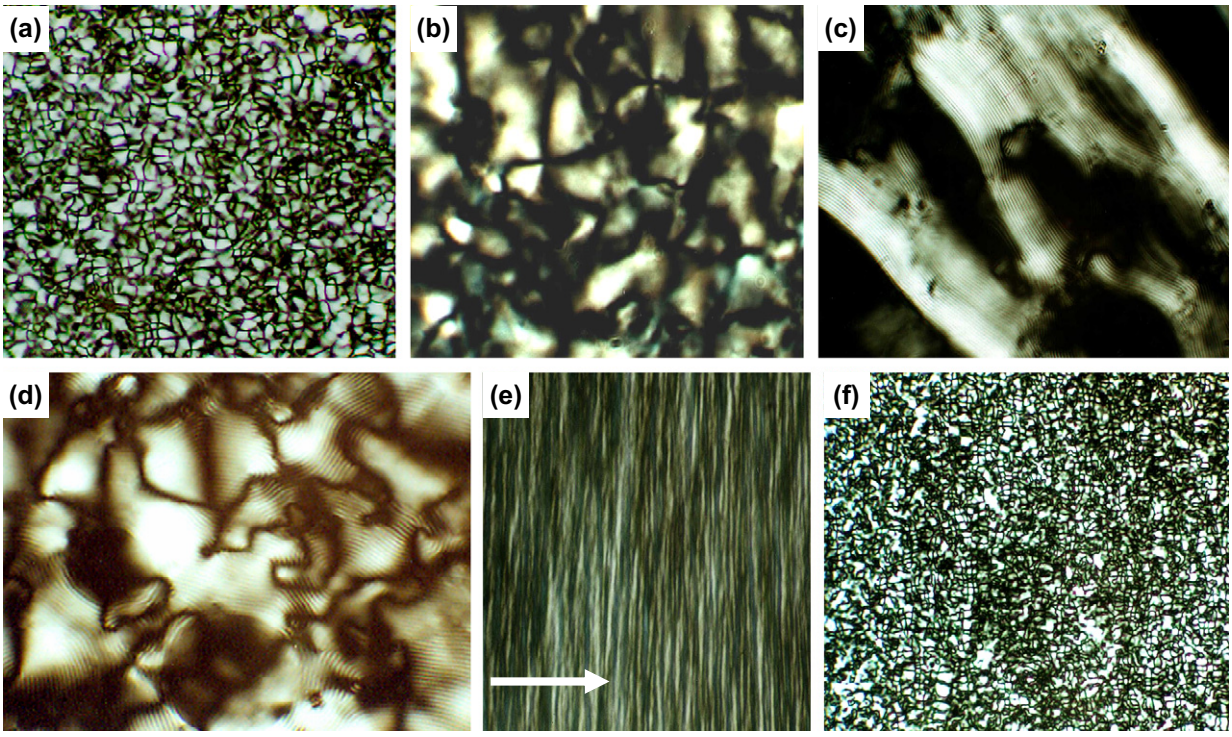

Fig. 4. Polarized light microscopic graphs of C_nPC texture (at 25 °C): (a) C_3PC 150×; (b) C_6PC 750×; (c) C_7PC 750×; (d) C_{10}PC 375×; (e) C_6PC 375×, arrow directs shear force direction; (f) C_2PC annealed at 150 °C for 20 min, 150×.

The cholesteric reflection peaks for C_3PC, C_4PC and C_5PC are 284 nm, 405 nm, and 673 nm, respectively. The insets in Fig. 5 are the blue and red optical images of samples with reflection peaks at 405 nm (for C_4PC) and 673 nm (for C_5PC), respectively. (For interpretation of the references to color in this figure, the reader is referred to the web version of this article.) The cholesteric reflections from C_6PC and C_7PC are located in the near infrared region. For example, C_6PC has a reflection peak at 1440 nm as shown in Fig. 5. In addition, the cholesteric reflection wavelength of C_{10}PC is estimated at around 2574 nm directly from the *d*-spacing of the uniform optical textures. The maximum reflection peak wavelength and the pitch distance of C_nPCs are listed in Table 2.

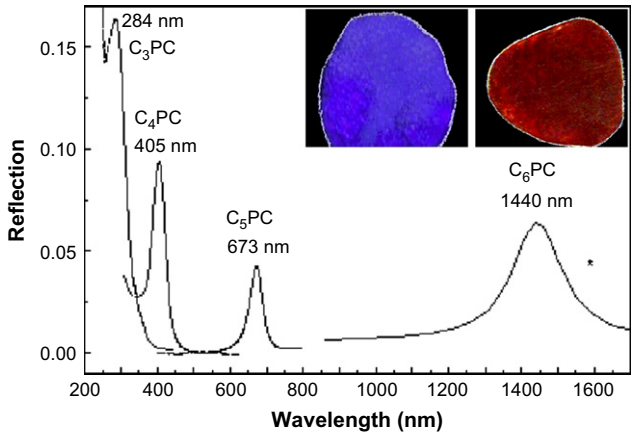

Fig. 5. Cholesteric reflection peaks for C_3PC, C_4PC, C_5PC and C_6PC at room temperature, measured using UV/vis/NIR photospectrometer in a reflection mode through 0.2-mm thick (C_3PC, C_4PC, C_5PC) and 1-mm thick (C_6PC) samples on glass substrates. The insets are the optical images of samples with reflections at 405 nm (for C_4PC) and 673 nm (for C_5PC), respectively.

The theory [1,25] emphasized that a maximum reflection peak wavelength was related to a pitch distance ($P_o \cos\theta = \lambda/n$, P_o stands for the pitch distance; n for average refractive index; λ for maximum reflection peak wavelength and $\cos\theta = 1$ when θ is the incident light along the normal direction). We find that the maximum reflection peak wavelength (λ) in this series of C_nPCs increases as the number of methylene units in the side chains increases as shown in Fig. 6b. Furthermore, the layer spacing is also a function of the number of methylene units in the side chains (see Fig. 6a). A twisting angle (φ) is defined as $\varphi = 360 \times d/P_o$ where d is the layer spacing which represents the distance of two adjacent layers in a helical structure of cholesteric liquid crystals. φ is calculated as a function of the length of side chains, as shown in Fig. 6c. The φ decreases with increasing numbers of methylene units. Furthermore, the number of layers in a periodic helical structure of the C_nPC cholesteric liquid crystals increases with the increase in the length of methylene units in the side chains of this series of C_nPCs (Fig. 6d). Therefore, it is concluded that the layer spacing, the pitch distance and the maximum reflection wavelength are associated with the length of methylene units in the cholesteric liquid crystal phase of C_nPCs.

4. Conclusion

A series of cholesteric LC polymers (C_nPC, $n = 5$, 6, 7 and 10) has been synthesized based upon the esterification of

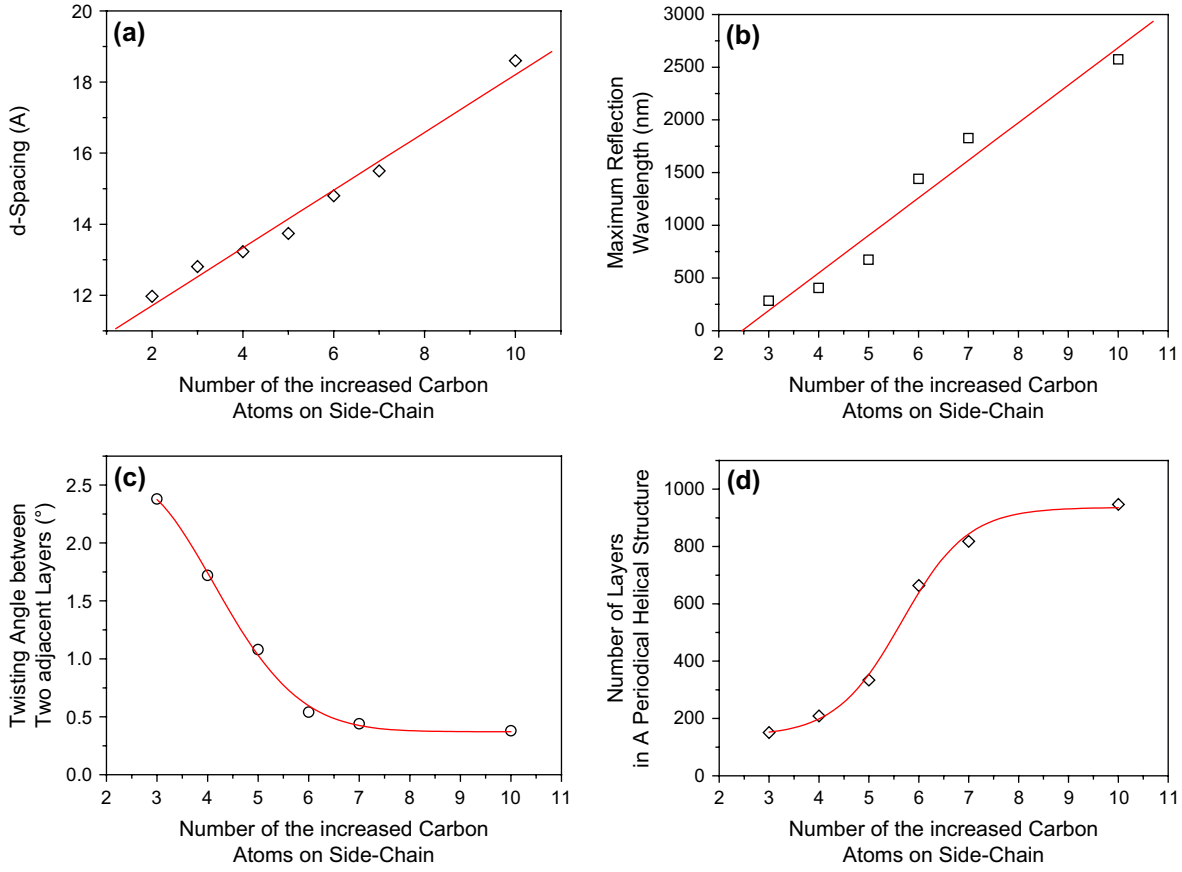

Fig. 6. (a) *d*-Spacing; (b) the maximum reflection peak wavelength; (c) the twisting angle between two adjacent layers; (d) number of layers in a periodical helical structure versus number of the increased carbon atoms on side-chain (substituted group).

cellulose molecules (HPCs) with aliphatic acid chloride. The number of methylene units (i.e., the side chain length) of the substituted aliphatyloxy groups possesses a significant influence on the selective reflection characteristics of the cholesteric liquid crystals in this series of C_nPC polymers. Increasing the number of methylene units in the side chains narrows the thermotropic phase transition window (between T_g and T_i) of C_nPC cholesteric liquid crystals. It is detected that the layer spacing of the cholesteric liquid crystals in this series of C_nPC polymers increases linearly with an increase in the methylene units in the side chains. It is observed that the maximum selective reflection peak wavelength and the corresponding pitch distance of the cholesteric LC phases (C_nPC) are strongly dependent on the number of methylene units in the side chains. Besides, the twisting angle φ and the layer number in the helical structure are also associated with the length of methylene units in the side chains of this series of C_nPC polymers.

References

[1] Wu ST, Yang DK. Reflective liquid crystal displays. New York: John Wiley & Sons; 2001.
[2] Yang DK, Wu ST. Fundamentals of liquid crystal devices. Auflage: John Wiley & Sons; 2006.
[3] Crawford GP. Flexible liquid crystal displays. New York: John Wiley & Sons; 2005.
[4] Crawford GP, Zumer S. Liquid crystals in complex geometries. London: Taylor and Francis; 1996.
[5] Gray DG. J Appl Polym Sci Appl Polym Symp 1983;37:179–80.
[6] Gilbert RD, Patton PA. Prog Polym Sci 1983;9:115–31.
[7] Isocai A, Ishizu A, Nakano J. J Appl Polym Sci 1985;30:345–53.
[8] Gray DG. Faraday Discuss Chem Soc 1985;79:257–60.
[9] Charlet G, Gray DG. Macromolecules 1987;20:33–8.
[10] Dave V, Frazier CE, Glasser WG. J Appl Polym Sci 1993;49:1671–8.
[11] Guo JX, Gray DG. Macromolecules 1989;22:2082–6.
[12] Kondo T, Sawatari C, Manley RStJ, Gray DG. Macromolecules 1994;27:210–5.
[13] Arai K, Satoh H. J Appl Polym Sci 1992;45:387–90.
[14] Navard P, Zachariades AE. J Polym Sci Part B Polym Phys 1987;25:1089–98.
[15] Ritcey AM, Gray DG. Macromolecules 1988;21:1251–5.
[16] Wang L, Huang Y. Macromolecules 2004;37:303–9.
[17] Ifuku S, Kamitakahara H, Takano T, Tanaka F, Nakatsubo F. Org Biomol Chem 2004;2:402–7.
[18] Teseng SL, Valente A, Gray DG. Macromolecules 1981;14:715–9.
[19] Tseng SL, Laivins GV, Gray DG. Macromolecules 1982;15:1262–4.
[20] Bhadani SN, Tseng SL, Gray DG. Macromol Chem 1983;184:1727–31.
[21] Laivins GV, Gray DG. Polymer 1985;26(9):1435–42.
[22] Bhadani SN, Gray DG. Mol Cryst Liq Cryst 1983;99:29–34.
[23] Ritcey AM, Holme KR, Gray DG. Macromolecules 1988;21:2914–7.
[24] Hou HQ, Reuning A, Wendorff JH, Greiner A. Macromol Chem Phys 2000;201:2050–4.
[25] Vries de HL. Acta Crystallogr 1951;4:219–26.